

## Raman Spectroscopic Characterization of Secondary Structure in Natively Unfolded Proteins: $\alpha$ -Synuclein

Nakul C. Maiti,<sup>†</sup> Mihaela M. Apetri,<sup>‡</sup> Michael G. Zagorski,<sup>‡</sup> Paul R. Carey,<sup>†,‡</sup> and Vernon E. Anderson<sup>\*,†,‡</sup>

*Contribution from the Departments of Biochemistry and Chemistry, Case Western Reserve University, Cleveland, Ohio 44106*

Received April 14, 2003; E-mail: vea@cwru.edu

**Abstract:** The application of Raman spectroscopy to characterize natively unfolded proteins has been underdeveloped, even though it has significant technical advantages. We propose that a simple three-component band fitting of the amide I region can assist in the conformational characterization of the ensemble of structures present in natively unfolded proteins. The Raman spectra of  $\alpha$ -synuclein, a prototypical natively unfolded protein, were obtained in the presence and absence of methanol, sodium dodecyl sulfate (SDS), and hexafluoro-2-propanol (HFIP). Consistent with previous CD studies, the secondary structure becomes largely  $\alpha$ -helical in HFIP and SDS and predominantly  $\beta$ -sheet in 25% methanol in water. In SDS, an increase in  $\alpha$ -helical conformation is indicated by the predominant Raman amide I marker band at 1654  $\text{cm}^{-1}$  and the typical double minimum in the CD spectrum. In 25% HFIP the amide I Raman marker band appears at 1653  $\text{cm}^{-1}$  with a peak width at half-height of  $\sim 33 \text{ cm}^{-1}$ , and in 25% methanol the amide I Raman band shifts to 1667  $\text{cm}^{-1}$  with a peak width at half-height of  $\sim 26 \text{ cm}^{-1}$ . These well-characterized structural states provide the unequivocal assignment of amide I marker bands in the Raman spectrum of  $\alpha$ -synuclein and by extrapolation to other natively unfolded proteins. The Raman spectrum of monomeric  $\alpha$ -synuclein in aqueous solution suggests that the peptide bonds are distributed in both the  $\alpha$ -helical and extended  $\beta$ -regions of Ramachandran space. A higher frequency feature of the  $\alpha$ -synuclein Raman amide I band resembles the Raman amide I band of ionized polyglutamate and polylysine, peptides which adopt a polyproline II helical conformation. Thus, a three-component band fitting is used to characterize the Raman amide I band of  $\alpha$ -synuclein, phosvitin,  $\alpha$ -casein,  $\beta$ -casein, and the non- $A\beta$  component (NAC) of Alzheimer's plaque. These analyses demonstrate the ability of Raman spectroscopy to characterize the ensemble of secondary structures present in natively unfolded proteins.

### Introduction

Natively unfolded proteins [The phrases intrinsically or natively unstructured/unfolded/denatured are used in the literature. We favor natively unfolded since it designates a set of conditions, i.e., native physiological conditions, where the protein is not folded into a compact defined conformation, and while these proteins are not folded into a compact form, the extent of residual structure may be variable.] are a growing class of proteins that do not adopt a unique conformation;<sup>1</sup> moreover, minimal secondary structure is observed by the standard methods of far UV circular dichroism or NMR. Tellingly, the hydrodynamic radii of these proteins are closer to that expected for random coils than for globular proteins. Taken together, these characterizations suggest that such proteins lack a defined structure, making the standard methods of structural biology irrelevant to understanding structure/function relationships. Thus, new methods of characterizing the ensemble of structures present are required. These methods, once developed, may also be

applied to the characterization of denatured proteins in order to understand the kinetics and thermodynamics of protein folding.<sup>2</sup>

Raman spectroscopy has the ability to provide a variety of probes into the structure of unfolded polypeptides. Raman studies of protein secondary structure have followed the approach taken by CD studies and focused on correlating the positions of the amide I and amide III vibrations with the crystallographically determined fraction of each secondary structural element present in globular proteins.<sup>3–6</sup> The latest analysis by Sane et al.<sup>6</sup> generated reference spectra for four different secondary structural elements that were successful at matching Raman spectra of globular proteins. However, this spectral decomposition did not reveal identifiable spectral contributions from the classical secondary structures.

Extrapolating empirical Raman parameters from globular proteins to natively unfolded proteins will presumably lead to significant errors, as some of the features that necessarily typify globular proteins are not present in natively unfolded proteins.

\* To whom correspondence should be addressed. Phone: (216) 368-2599. Fax: (216) 368-3419.

<sup>†</sup> Department of Biochemistry.

<sup>‡</sup> Department of Chemistry.

(1) Uversky, V. N. *Eur. J. Biochem.* **2002**, *269*, 2.

(2) Smith, C. R.; Mateljevic, N.; Bowler, B. E. *Biochemistry* **2002**, *41*, 10173.

(3) Williams, R. W. *Methods Enzymol.* **1986**, *130*, 311.

(4) Marx, J.; Berjot, M.; Alix, A. J. *J. Raman Spectrosc.* **1987**, *18*, 289.

(5) Miura, T.; Thomas, G. J., Jr. *Subcell. Biochem.* **1995**, *24*, 55.

(6) Sane, S. U.; Cramer, S. M.; Przybycien, T. M. *Anal. Biochem.* **1999**, *269*, 255.

There are two prominent differences. First, natively unfolded proteins are not constrained to have their polypeptide backbone reverse direction to maintain a globular structure. The release of this constraint is apparent in the increased hydrodynamic radii of natively unfolded proteins. Second, natively unfolded proteins have a more consistent solvent exposure of the amide bonds due to the absence of a hydrophobic core. This enhanced solvent accessibility can be revealed by rapid amide proton exchange, as observed in  $\alpha$ -synuclein.<sup>7,8</sup> In this contribution, we employ  $\alpha$ -synuclein as a model for natively unfolded proteins since it can be induced to adopt both extensive  $\alpha$ -helical and  $\beta$ -sheet conformations. We show that Raman spectroscopy can serve as a basis for characterizing changes in conformational states induced by environmental changes and for identifying the conformational constituents of proteins that are unfolded.

Raman spectroscopy enjoys several important advantages in characterizing the vibrational spectra and secondary structural tendencies of natively unfolded proteins. Raman spectra can be obtained in dilute aqueous solution,<sup>9,10</sup> a virtue that is of enhanced importance in characterizing natively unfolded proteins because of their tendency to aggregate at higher concentrations. The H<sub>2</sub>O bending vibration mode that obscures the amide I band in IR spectroscopy has a low intensity in the Raman spectra, obviating the need to use D<sub>2</sub>O, and reduces the errors inherent in large background solvent subtractions. Raman spectroscopic characterization can be applied to proteins in varied states: aqueous solutions, precipitated fibrils, amorphous aggregates,<sup>11–14</sup> solids,<sup>15</sup> and crystals.<sup>6,16–18</sup> These spectra can be directly compared, which will allow the comparison of the protein conformations present in these states. This becomes of significant importance in understanding the pathways of protein aggregation in vitro and in vivo. In addition to the characterization of the amide I and other amide bands, there are additional features in the Raman spectra that permit the environment of numerous amino acid side chains to be characterized, including the aromatic amino acids,<sup>6,19</sup> the acidic residues,<sup>20</sup> and sulfur-containing residues<sup>5,13,16,21</sup> in the different physical states.

$\alpha$ -Synuclein, an abundant small (140 amino acids) presynaptic protein of uncertain function, belongs to a larger family of proteins including  $\beta$ - and  $\gamma$ -synuclein.<sup>22</sup> The synucleins are prototypical members of the class of natively unfolded proteins,<sup>23</sup> but only  $\alpha$ -synuclein is prone to fibrillization.<sup>24</sup> Interest in  $\alpha$ -synuclein has increased because it is the major component

of Lewy bodies, the intracytoplasmic inclusions that are the neuropathological hallmark of Parkinson's disease.<sup>25,26</sup> Additionally, two mutations (A53T and A30P) in the gene encoding  $\alpha$ -synuclein have been linked to familial early-onset Parkinson's disease.<sup>27,28</sup>

The identification of  $\alpha$ -synuclein as being natively unfolded is well documented by circular dichroism (CD) [Abbreviations used: BWHH, fitted bandwidth at half-height; CD, circular dichroism; HFIP, hexafluoro-2-propanol; NAC, non-amyloid- $\beta$  peptide component of Alzheimer's disease plaques; PWHH, experimental peak width at half-height; ROA, Raman optical activity; SDS, sodium dodecyl sulfate; TFA, trifluoroacetic acid], Fourier transform infrared, and NMR spectroscopy, substantiating the assessment that  $\alpha$ -synuclein has "little or no" secondary structure in aqueous solution.<sup>23,29</sup> Raman optical activity (ROA) studies have suggested that a fraction of the extended structure is polyproline II.<sup>30,31</sup> However,  $\alpha$ -synuclein can adopt different conformations, becoming  $\alpha$ -helical when bound to micelles or phospholipids<sup>7,8,23,32</sup> or in the presence of fluorinated solvent<sup>23,33,34</sup> and forming a  $\beta$ -sheet structure in the presence of alcohols<sup>34,35</sup> or allowing the formation of fibrils at low pH.<sup>36–38</sup> In neutral aqueous solution the random structure slowly rearranges into soluble and aggregated  $\beta$ -sheet structures that eventually precipitate as amyloid.<sup>39–41</sup>

Since different conditions induce  $\alpha$ -synuclein to adopt predominantly  $\beta$ -sheet or  $\alpha$ -helical conformations, we have the opportunity to use a single protein to characterize features in the Raman spectra that are associated with these secondary structures. Analysis of the Raman spectra of  $\alpha$ -synuclein in these different conformations provides "basis spectra" that may be used to characterize changes in the ensemble of conformations present in solutions of native  $\alpha$ -synuclein. A simple three-component band fitting of the amide I band using these basis functions is proposed and applied to additional natively unfolded proteins.

- (7) Eliezer, D.; Kutluay, E.; Bussell, R., Jr.; Browne, G. J. *Mol. Biol.* **2001**, *307*, 1061.
- (8) Chandra, S.; Chen, X.; Rizo, J.; Jahn, R.; Sudhof, T. C. *J. Biol. Chem.* **2003**.
- (9) Dong, J.; Dinakarpanian, D.; Carey, P. R. *Appl. Spectrosc.* **1998**, *52*, 1117.
- (10) Pelton, J. T.; McLean, L. R. *Anal. Biochem.* **2000**, *277*, 167.
- (11) Yu, N. T.; Jo, B. H.; Chang, R. C.; Huber, J. D. *Arch. Biochem. Biophys.* **1974**, *160*, 614.
- (12) Miura, T.; Suzuki, K.; Kohata, N.; Takeuchi, H. *Biochemistry* **2000**, *39*, 7024.
- (13) Dong, J.; Atwood, C. S.; Anderson, V. E.; Siedlak, S. L.; Smith, M. A.; Perry, G.; Carey, P. R. *Biochemistry* **2003**, *42*, 2768.
- (14) Dong, J.; Wan, Z.; Popov, M.; Carey, P. R.; Weiss, M. A. *J. Mol. Biol.* **2003**, *330*, 431.
- (15) Chen, M. C.; Lord, R. C. *J. Am. Chem. Soc.* **1974**, *96*, 4750.
- (16) Honzatko, R. B.; Williams, R. W. *Biochemistry* **1982**, *21*, 6201.
- (17) Smulevich, G.; Spiro, T. G. *Methods Enzymol.* **1993**, *226*, 397.
- (18) Altose, M. D.; Zheng, Y.; Dong, J.; Palfey, B. A.; Carey, P. R. *Proc. Natl. Acad. Sci. U.S.A.* **2001**, *98*, 3006.
- (19) Overman, S. A.; Thomas, G. J., Jr. *Biochemistry* **1995**, *34*, 5440.
- (20) Overman, S. A.; Thomas, G. J., Jr. *Biochemistry* **1999**, *38*, 4018.
- (21) Rajkumar, B. J.; Ramakrishnan, V. *Spectrochim. Acta, Part A: Mol. Biomol. Spectrosc.* **2001**, *57*, 247.
- (22) Maroteaux, L.; Scheller, R. H. *Brain Res. Mol. Brain Res.* **1991**, *11*, 335.
- (23) Weinreb, P. H.; Zhen, W.; Poon, A. W.; Conway, K. A.; Lansbury, P. T., Jr. *Biochemistry* **1996**, *35*, 13709.
- (24) Uversky, V. N.; Li, J.; Souillac, P.; Millett, I. S.; Doniach, S.; Jakes, R.; Goedert, M.; Fink, A. L. *J. Biol. Chem.* **2002**, *277*, 11970.
- (25) Spillantini, M. G.; Schmidt, M. L.; Lee, V. M.; Trojanowski, J. Q.; Jakes, R.; Goedert, M. *Nature* **1997**, *388*, 839.
- (26) Spillantini, M. G.; Crowther, R. A.; Jakes, R.; Hasegawa, M.; Goedert, M. *Proc. Natl. Acad. Sci. U.S.A.* **1998**, *95*, 6469.
- (27) Polymeropoulos, M. H.; Lavedan, C.; Leroy, E.; Ide, S. E.; Dehejia, A.; Dutra, A.; Pike, B.; Root, H.; Rubenstein, J.; Boyer, R.; Stenroos, E. S.; Chandrasekharappa, S.; Athanassiadou, A.; Papapetropoulos, T.; Johnson, W. G.; Lazzarini, A. M.; Duvoisin, R. C.; Di Iorio, G.; Golbe, L. I.; Nussbaum, R. L. *Science* **1997**, *276*, 2045.
- (28) Kruger, R.; Kuhn, W.; Muller, T.; Woitalla, D.; Graeber, M.; Kosel, S.; Przuntek, H.; Epplen, J. T.; Schols, L.; Riess, O. *Nat. Genet.* **1998**, *18*, 106.
- (29) Eliezer, D.; Kutluay, E.; Bussell, R., Jr.; Browne, G. J. *Mol. Biol.* **2001**, *307*, 1061.
- (30) Bochicchio, B.; Tamburro, A. M. *Chirality* **2002**, *14*, 782.
- (31) Syme, C. D.; Blanch, E. W.; Holt, C.; Jakes, R.; Goedert, M.; Hecht, L.; Barron, L. D. *Eur. J. Biochem.* **2002**, *269*, 148.
- (32) Bussell, R., Jr.; Eliezer, D. *J. Biol. Chem.* **2001**, *276*, 45996.
- (33) Li, H. T.; Du, H. N.; Tang, L.; Hu, J.; Hu, H. Y. *Biopolymers* **2002**, *64*, 221.
- (34) Munishkina, L. A.; Phelan, C.; Uversky, V. N.; Fink, A. L. *Biochemistry* **2003**, *42*, 2720.
- (35) Boodles, A. M.; Guthrie, D. J.; Harriott, P.; Campbell, P.; Irvine, G. B. *Eur. J. Biochem.* **2000**, *267*, 2186.
- (36) Conway, K. A.; Harper, J. D.; Lansbury, P. T., Jr. *Biochemistry* **2000**, *39*, 2552.
- (37) Uversky, V. N.; Li, J.; Fink, A. L. *J. Biol. Chem.* **2001**, *276*, 10737.
- (38) Uversky, V. N.; Lee, H. J.; Li, J.; Fink, A. L.; Lee, S. J. *J. Biol. Chem.* **2001**, *276*, 43495.
- (39) El-Agnaf, O. M.; Boodles, A. M.; Guthrie, D. J.; Harriott, P.; Irvine, G. B. *Eur. J. Biochem.* **1998**, *258*, 157.
- (40) Serpell, L. C.; Berriman, J.; Jakes, R.; Goedert, M.; Crowther, R. A. *Proc. Natl. Acad. Sci. U.S.A.* **2000**, *97*, 4897.
- (41) Hu, H. Y.; Li, Q.; Cheng, H. C.; Du, H. N. *Biopolymers* **2001**, *62*, 15.

## Materials and Methods

**Chemicals.** Methanol was purchased from Fischer Scientific. Hexafluoro-2-propanol, deuterium oxide (99.8%, D<sub>2</sub>O), and deuterium chloride (DCI) were obtained from Aldrich Chemical. Sodium dodecyl sulfate (SDS) was obtained from Boehringer Mannheim Corp. Phosvitin,  $\alpha$ -casein, and  $\beta$ -casein were obtained from Sigma Chemical and used without further purification. Milli Q ultrapurified deionized water was used for sample preparation. NAC (nonamyloid- $\beta$  peptide component of Alzheimer's plaques, EQVTNVGGAVVTGVTAVAQKTVEGAG-SIAAATGFV) was synthesized on an Applied Biosystems 433A peptide synthesizer using standard Fmoc protocols with Val-PEG-PG resin and *N*-[(dimethylamino)-1*H*-1,2,3-triazolo[4,5-*b*]pyridino-1-ylmethylene]-*N*-methylm ethanaminium hexafluorophosphate *N*-oxide as the coupling reagent. The peptide was cleaved from the resin using trifluoroacetic acid (TFA) followed by precipitation and washing repeatedly with diethyl ether. The crude peptide was purified by RP-HPLC (C18 column, Zorbax) with a solvent gradient consisting of TFA/water/acetonitrile (0.1/95/4.9 and 0.1/4.9/95, over a period of 40 min). The purified peptide was lyophilized and stored at  $-70$  °C. The peptide identity was confirmed by MALDI-ToF as being  $m/z = 3261$ .

**Expression and Purification of  $\alpha$ -Synuclein.**  $\alpha$ -Synuclein was overexpressed in *E. coli* BL21(DE3) using plasmid pT7-7, containing the gene for wild-type human  $\alpha$ -synuclein, provided by Dr. Peter Lansbury's laboratory (Harvard Medical School, Cambridge, MA). Expression and purification followed the previously published protocol.<sup>36</sup> Cells were grown in Luria Broth in the presence of ampicillin (100  $\mu$ g/mL), and  $\alpha$ -synuclein expression was induced by the addition of 1 mM isopropyl  $\beta$ -D-isopropylthiogalactopyranoside. The bacterial pellet was resuspended in lysis buffer (10 mM Tris pH 8.0, 1 mM ethylenediaminetetraacetate, 1 mM phenylmethanesulfonyl fluoride, 1 mM dithiothreitol) followed by sonication and centrifugation at 10 000 rpm for 30 min. A streptomycin sulfate and two ammonium sulfate precipitations were used for further purification of  $\alpha$ -synuclein, with the protein being stored after the final ammonium sulfate precipitation. The pellet was resuspended in 10 mM Tris-HCl (pH 7.4), 1 mM phenylmethanesulfonyl fluoride, loaded onto a diethylaminoethyl column, and eluted with a NaCl gradient. The relevant fractions (judged by MALDI-ToF mass spectrometry) were pooled, and protein was precipitated by addition of ammonium sulfate and stored at  $-80$  °C.

**Sample Preparation for Spectroscopy.** Before each set of experiments, precipitated  $\alpha$ -synuclein was dissolved in 20 mM Tris-HCl, pH 7.5, centrifuged at 16 000g for 2 min to remove any insoluble particles and loaded onto a 2.5  $\times$  50 cm Sephacryl S-200 HR, GF column (Amersham Pharmacia) equilibrated with buffer. The monomer peak was collected, and protein was concentrated to  $\sim 300$   $\mu$ M using a Millipore Amicon Ultra 10 kDa concentrator. Protein concentrations were determined by UV absorbance measurements using an estimated extinction coefficient of 5800 M<sup>-1</sup>cm<sup>-1</sup> at 276 nm, the  $\alpha$ -synuclein purity was judged by the presence of a single band by Native/PAGE, and the  $M_r$  of 14 460 confirmed by mass spectrometry. For both CD and Raman studies, 200  $\mu$ M  $\alpha$ -synuclein in 20 mM Tris-HCl buffer (pH 7.5) was used in all solutions. Solutions of  $\alpha$ -casein,  $\beta$ -casein, and phosvitin were prepared by dissolving the proteins to a concentration of 10 mg/mL in water. The pH was maintained at 7.5 by addition of NaOH, as required. NAC (3 mg/mL) was dissolved in 20 mM Tris-HCl buffer (pH 7.5).

**CD Spectroscopy.** Far UV-CD measurements were performed at 23 °C on a Jasco J-810 spectropolarimeter using an  $\alpha$ -synuclein concentration of 200  $\mu$ M. Spectra were recorded using a 0.1 mm path length cell from 190 to 250 nm with a 50 nm/min scan speed and a 2 s response time. For each sample three scans were averaged and the buffer background subtracted. CD spectra were deconvoluted using the learning neural network program K2D.<sup>42</sup> Other programs, CDANAL,<sup>43</sup>

SELCON,<sup>44</sup> CDSSTR, and CONTIN,<sup>45,46</sup> were also utilized with significantly different results.

**Infrared Measurement.** IR spectra of  $\sim 200$   $\mu$ M  $\alpha$ -synuclein in D<sub>2</sub>O buffer (20 mM Tris-DCI, pH 7.5) were obtained with a Bruker IFS 66 spectrometer using a 0.05 mm path length and CaF<sub>2</sub> windows.

**Raman Spectroscopy.** Raman spectra were obtained using 647.1 nm Kr<sup>+</sup> laser excitation with 90° excitation/collection geometry and a Holospec f/1.4 axial transmission spectrometer (Kaiser Optical Systems, Inc.) employed as a single monochromator, as described previously.<sup>9</sup> The detection system utilized a back-illuminated charge-coupled device detector (Princeton Instruments, Inc.). A 50  $\mu$ L amount of protein samples was held in a 2  $\times$  2 mm quartz cuvette. Data were acquired using a laser power of  $\sim 800$  mW with spectral acquisition times of 5 min. In the presence of cosolvents, the spectra were, in some cases, both time and concentration dependent.  $\alpha$ -Synuclein (200  $\mu$ M) and spectral acquisition within 5–10 min of the addition of cosolvent minimized variability. Buffer/solvent spectra in the 400–1900 cm<sup>-1</sup> range were subtracted from the protein solution spectra. Three to five solvent-corrected spectra were averaged to give the final spectra to display in the figures. While there is no internal standard to monitor the solvent subtraction, we recorded the solvent spectra under identical conditions. The entire range (400–1900 cm<sup>-1</sup>) of the subtracted spectra was monitored for the proper solvent subtraction. In a few cases excess buffer bands (due to small variation of the buffer concentration) were removed by subtracting the buffer-only spectra. External wavenumber calibration yields Raman band positions to within  $\pm 1$  cm<sup>-1</sup> for sharp bands. Data analysis was performed using GRAMS/32 software (Galactic Industries, Inc.).

**Curve Fitting of the Amide I Profile.** Band fitting of the Raman amide I mode (1590–1720 cm<sup>-1</sup>) of  $\alpha$ -synuclein and other proteins was performed with the CurveFit.Ab routine of GRAMS/32, which is based on the Levenberg–Marquardt nonlinear least-squares method.<sup>47</sup> The advanced AutoFind peak picker selected three peaks in the amide I region with a 25 cm<sup>-1</sup> bandwidth at half-height (BWHH). This choice of bandwidth was based on the experimental peak widths observed for highly regular  $\alpha$ -helix or  $\beta$ -sheet subunits. A mixed Gaussian and Lorentzian peak shape was employed. Two bands at  $\sim 1604$  and  $\sim 1615$  cm<sup>-1</sup>, due to ring modes from aromatic side chains, were included with the amide I bands during the curve fitting process since they were not baseline separated from the amide I feature. The baseline from 1590 to 1720 cm<sup>-1</sup> was assumed to be linear. In addition to the described three-component fit, we tested two- and four-component fits. Comparisons of the  $\chi^2$  values and the residuals of the fits were used as the criteria for assessing the quality of fit.

## Results

**Native  $\alpha$ -Synuclein.** The Raman spectrum in the region of 600–1800 cm<sup>-1</sup> of  $\alpha$ -synuclein in 20 mM Tris-HCl, pH 7.5, is shown in Figure 1a and the vibrational modes listed in Table 1. The Raman spectrum has a broad amide I band at 1674 cm<sup>-1</sup> with a peak width at half-height (PWHH) of  $\sim 50$  cm<sup>-1</sup>. The peak width and the asymmetry of the amide I band suggest a distribution of secondary structures. Band fitting revealed two shoulder bands near 1665 and 1653 cm<sup>-1</sup>. The band at 1665 cm<sup>-1</sup> is a marker band for  $\beta$ -sheet, as typified, by, e.g., *Bombix* silk,<sup>48</sup> and the shoulder at 1653 cm<sup>-1</sup> is a marker band associated with  $\alpha$ -helical peptide bonds.<sup>49–54</sup> The conformationally infor-

(43) Perczel, A.; Park, K.; Fasman, G. D. *Anal. Biochem.* **1992**, *203*, 83.

(44) Sreerama, N.; Woody, R. W. *Anal. Biochem.* **2000**, *287*, 252.

(45) Sreerama, N.; Woody, R. W. *Anal. Biochem.* **1993**, *209*, 32.

(46) Provencher, S. W.; Glockner, J. *Biochemistry* **1981**, *20*, 33.

(47) Marquardt, D. W. *J. Soc. Ind. Appl. Math.* **1963**, *11*, 431.

(48) Shao, Z.; Vollrath, F.; Sirichaisit, J.; Young, R. J. *Polymer* **1999**, *40*, 2493.

(49) Miura, T.; Thomas, G. J., Jr. *Subcell. Biochem.* **1995**, *24*, 55.

(50) Laporte, L.; Stultz, J.; Thomas, G. J., Jr. *Biochemistry* **1997**, *36*, 6, 8053.

(51) Krimm, S.; Bandekar, J. *Adv. Protein Chem.* **1986**, *38*, 181.

(42) Andrade, M. A.; Chacon, P.; Merelo, J. J.; Moran, F. *Protein Eng.* **1993**, *6*, 383.



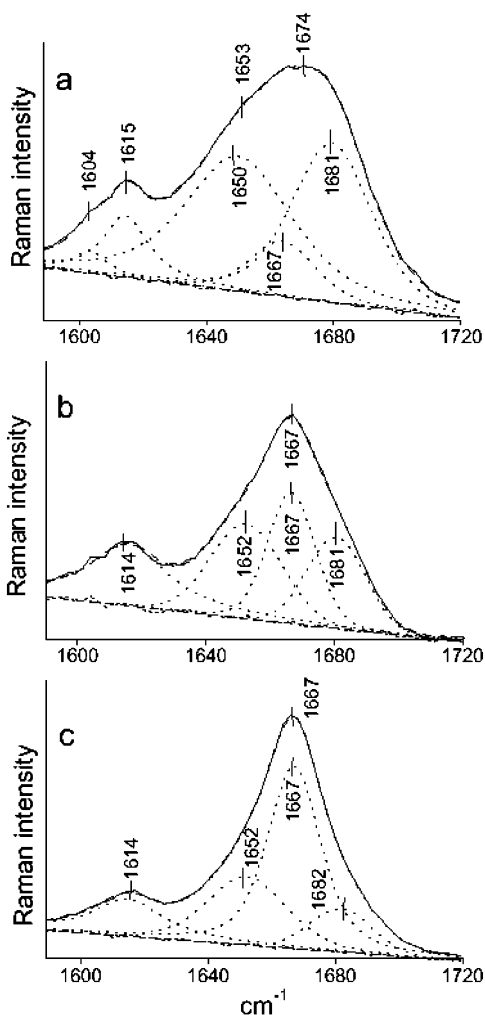


**Figure 3.** Curve fitting of the amide I vibration mode of  $\alpha$ -synuclein (0.2 mM) in 20 mM Tris-HCl and in the presence of different concentrations of methanol: (a) 0% methanol, (b) 17.5% methanol, and (c) 25.0% methanol. The dotted lines denote individual component functions and the solid lines the sum of the functions. The dashed lines are the experimentally determined spectra. Baseline (segmented) and the residual (short dashes along with the baseline) are also shown in the figure. The peak positions are marked.

bands at 208 and 222 nm (Figure 4d) typical of  $\alpha$ -helical proteins. In 25% HFIP the amplitudes of the negative minima are increased by 64% relative to that observed in the presence of SDS (Figure 4b), consistent with the enhanced 1654 cm<sup>-1</sup> band in the Raman spectrum. The CD spectrum of  $\alpha$ -synuclein in 25% HFIP establishes its predominantly  $\alpha$ -helical conformation.

**Amide I Band Fitting.** Both the amide I and amide III bands of native  $\alpha$ -synuclein at pH 7.5 are broad, indicating a mixture of conformations. For the amide I region, a simple curve-fitting technique was applied to dissect the contributions from different secondary conformations. The presence of three amide I bands constrained at  $\sim 1650$ – $1656$ ,  $\sim 1664$ – $1670$ , and  $\sim 1680$  cm<sup>-1</sup> were assumed. On the basis of the SDS and HFIP spectra, the  $\sim 1654$  cm<sup>-1</sup> band derives from  $\alpha$ -helical conformations. On the basis of the response of the spectra to increasing methanol concentrations, the  $\sim 1667$  band has contributions from  $\beta$ -sheet structures. These peaks were characterized by BWHH < 40 cm<sup>-1</sup>, which was adopted as an additional constraint to the band fits. In the absence of cosolvents, the amide I spectra of  $\alpha$ -synuclein and other random structure proteins and polypep-

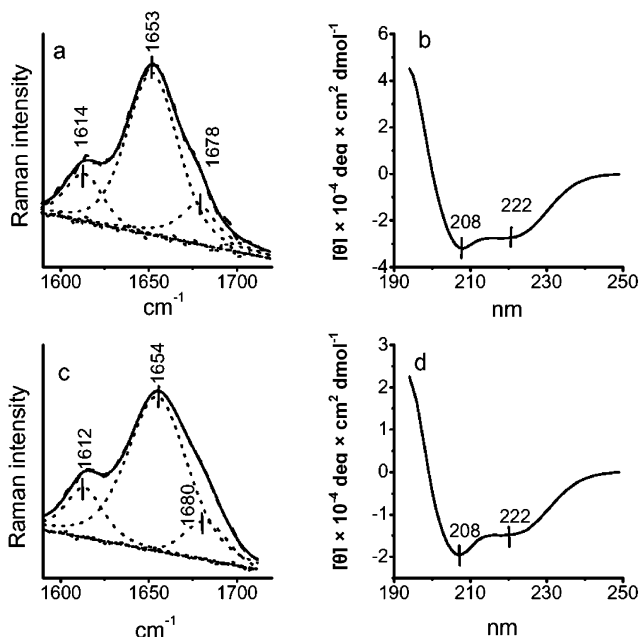


**Figure 4.** The 647.1 nm excited Raman spectra (amide I region, 1590–1725 cm<sup>-1</sup>) of  $\alpha$ -synuclein (0.2 mM, 20 mM Tris-HCl buffer, pH 7.5) in 25% HFIP (a) and in 1% SDS solution (c). The spectra were band fitted, and each component band is shown as a dotted line. Baseline (segmented) and residuals of the fit (short dashes along with the baseline) are also shown. Curve b shows the CD spectra of the same protein solution in the presence of 1% SDS and d in the presence of 25% HFIP.

tides have maxima at higher frequencies (1674–1685 cm<sup>-1</sup>, Figures 5 and 6a, b) indicating the presence of a band at higher frequency than the characteristic  $\beta$ -sheet and  $\alpha$ -helix marker bands. Two bands at 1604 and 1615 cm<sup>-1</sup> need to be included in the band-fitting protocol to account for ring modes from aromatic residues. As shown in Figure 3a, these three bands are sufficient to reproduce the amide I feature. A two-band protocol with no constraints fails to fit the band, while four-band protocols do not significantly reduce  $\chi^2$ .

An advantage of this fitting protocol is that it permits the quantitation of the component bands in a spectrum. The integrated areas from the band-fitting procedure are tabulated in Table 2. The fit of the amide I peak of  $\alpha$ -synuclein in 0% methanol shows that the major intensity is found in the component bands at 1650 (48%) and 1681 cm<sup>-1</sup> (37%), while the component band at 1669 cm<sup>-1</sup> makes only a minor contribution. Analysis of  $\alpha$ -synuclein in 17.5% methanol shows three-component bands close to the positions observed for  $\alpha$ -synuclein in 0% methanol (Figure 3b and Table 2); however, the intensity pattern of the bands changes. The intensity of the higher and lower frequency bands decreases with the band at 1667 cm<sup>-1</sup> increasing. In higher concentrations of methanol ( $\geq 25\%$ ), the 1667 cm<sup>-1</sup> band predominates, accounting for over 70% of the amide I band intensity, and narrows so that the BWHH is 25 cm<sup>-1</sup> (Figure 3c). The coalescence of the amide I peak into a single narrow peak suggests a common conformation for the majority of the peptide bonds.

The curve-fitting technique was applied for the conformational analysis of phosvitin,  $\alpha$ -casein,  $\beta$ -casein, and NAC. Figure 5 shows the curve fitting for amide I bands for these proteins, and the results are shown in Table 2. While all of these proteins are reported to be natively unfolded, there are significant differences in the amide I band, suggesting that there are

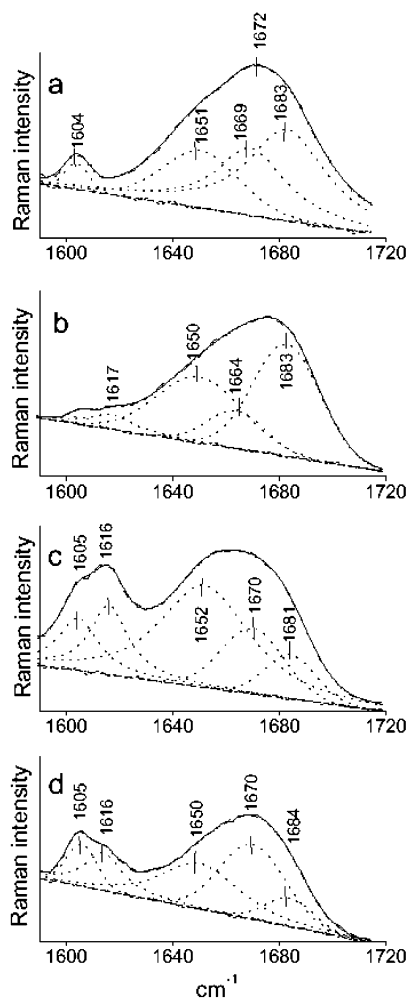


**Figure 5.** Curve fitting of the amide I vibration mode of NAC (a), phosvitin (b),  $\alpha$ -casein (c), and  $\beta$ -casein (d). The spectra obtained at 647.1 nm excitation and the other experimental conditions are the same as those in Figure 1 and as described in the Materials and Methods section. The dotted lines denote individual component functions and the solid lines the sum of the functions. The dashed lines are the experimentally determined spectra. Baseline (segmented) and the residual (short along with the baseline) are also shown in the figure. The peak positions are marked.

differences in backbone conformational preferences. The success of the three-component fitting procedure is evident from the absence of any significant deviation between the fitted and observed spectra. The differences apparent in the spectra are quantified by the band-fitting procedure to permit a correlation with secondary structural preference.

**Correlation of Raman Band Intensities with Conformational States.** To correlate the integrated band intensities of the amide I peak with the fraction of each secondary structure, the assumption is made that the Raman cross section of each conformation is identical. The errors inherent to this approach have been discussed by Surewicz<sup>60</sup> and Sane et al.<sup>6</sup> The validity of the assumption that the Raman cross section for each band is nearly identical can be experimentally approached by determining the ratio of the amide I peak with a second Raman peak that is not a function of secondary structure. The differences in scattering efficiency for different secondary structures obtained by Sane et al.<sup>6</sup> vary by less than a factor of

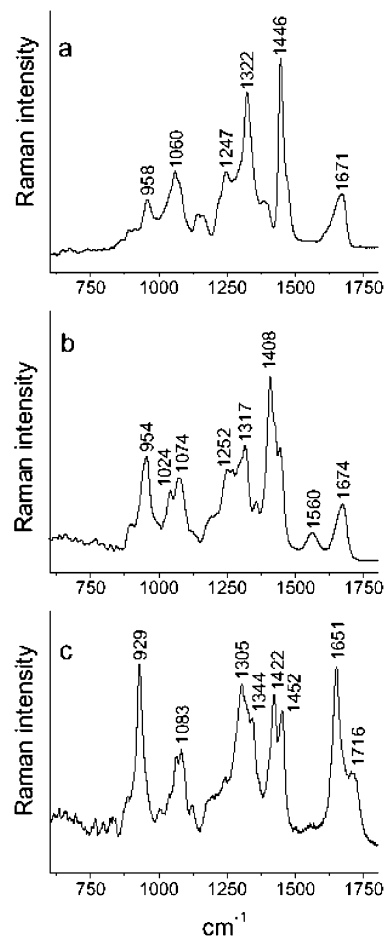


**Figure 6.** The 647.1 nm excited Raman spectra (600–1800  $\text{cm}^{-1}$ ) of poly-L-glutamic acid (1 mM) and poly-L-lysine (1 mM) at different pH values: (a) fully protonated poly-L-lysine at pH 3.5, (b) fully ionized poly-L-glutamic acid at pH 12.1, and (c) poly-L-glutamic acid at pH 3.5. The other experimental conditions were the same as those in Figure 1. The major bands are marked in the spectrum.

<sup>2,6</sup> Table 3 shows the normalized amide I band intensity for  $\alpha$ -synuclein with respect to the tyrosine band at  $\sim 1615 \text{ cm}^{-1}$  under all experimental conditions. The addition of cosolvents varied the relative integrated area of any of the three resolved bands from  $<10\%$  to over  $50\%$ , while the integrated area of the entire amide I peak relative to the Tyr ring band at  $\sim 1615 \text{ cm}^{-1}$  varied only  $\pm 30\%$ . If the amide I bands from different secondary structures had significantly different Raman cross sections, then the ratio of the amide I band to the Tyr ring mode (that is independent of secondary structure) would necessarily reveal that change. The minimal change of this intensity ratio suggests that the integrated amide I band areas should provide a semiquantitative estimate of the secondary structure composition.

**Side Chain Specific Raman Features.** The Raman spectra of proteins usually display sharp features due to aromatic ring modes. In  $\alpha$ -synuclein the Tyr Fermi doublet appears at 830 and  $853 \text{ cm}^{-1}$ . In 25% methanol the intensity ratio and the positions of these bands are effectively unchanged, though their PWHH decreased in the presence of methanol. In SDS micelles, the Tyr Fermi doublet is again at 829 and  $856 \text{ cm}^{-1}$  (Figure 1). The intensity ratio increased slightly. The consistency of these features suggests that the H-bonding environment of the Tyr

(60) Surewicz, W. K.; Mantsch, H. H.; Chapman, D. *Biochemistry* **1993**, *32*, 389.

**Table 2.** Curve Fitting of the Amide I Mode of Different Proteins and Peptides<sup>a</sup>

peak no.	center	width	% area
$\alpha$ -synuclein in Tris buffer, 0% methanol			
1	1650 (6)	40 (L)	48
2	1667 (5)	26 (16)	15
3	1681 (3)	29 (3)	37
$\alpha$ -synuclein in Tris buffer, 17.5% methanol			
1	1652 (6)	26 (6)	34
2	1667 (1)	18 (5)	39
3	1681 (4)	21 (4)	27
$\alpha$ -synuclein in Tris buffer, 25% methanol			
1	1652 (7)	29 (7)	20
2	1667 (1)	20 (6)	70
3	1682 (7)	23 (8)	10
NAC in Tris buffer, pH 7.5			
1	1651 (3)	34 (5)	24
2	1669 (2)	31 (11)	31
3	1683 (2)	35 (4)	49
phosvitin in water pH 7.5			
1	1650 (L)	38 (1)	37
2	1664 (2)	26 (4)	14
3	1683 (1)	30 (1)	49
$\alpha$ -casein in water, pH 7.5			
1	1653 (7)	39 (4)	63
2	1670 (L)	28 (20)	25
3	1684 (1)	22 (2)	12
$\beta$ -casein in water, pH 7.5			
1	1650 (6)	34 (4)	39
2	1670 (L)	29 (9)	48
3	1684 (1)	21 (3)	13

<sup>a</sup> Values in parenthesis are the standard error. L: the parameter reached one of the limits.

**Table 3.** The Normalized Amide I Band Intensity of  $\alpha$ -Synuclein with Respect to an Intrinsic Tyr Band

	0% MeOH	17.5% MeOH	25% MeOH	1% SDS	25% HFIP
Tyr area (1615 cm <sup>-1</sup> )	19	6	3	18	4
amide I area (1640–1690 cm <sup>-1</sup> )	130	33	23	85	35
ratio (amide I/Tyr)	6.9	5.3	7.6	5.7	8.6

OH is not altered significantly by the change in conformation induced by the addition of methanol or SDS.

$\alpha$ -Synuclein contains 6 Asp and 18 Glu residues largely in the acidic C-terminal domain of the protein. The side chain carboxylic acid groups of Asp or Glu when protonated have characteristic C=O stretching bands between 1720 and 1770 cm<sup>-1</sup> in the Raman spectrum and a symmetric carboxylate (CO<sub>2</sub><sup>-</sup>) stretching band at 1360–1450 cm<sup>-1</sup> when ionized.<sup>61</sup> In Figure 1a the Raman band appears at ~1403 cm<sup>-1</sup>, while no assignable bands were observed in the 1720–1770 cm<sup>-1</sup>, indicating that the carboxylate groups remain largely ionized in all of the methanol solvent conditions examined. The same conclusion can be drawn from the SDS micelles data (Figure 1c)

## Discussion

**Conformations of Natively Unfolded Proteins.** Natively unfolded proteins have become of considerable interest as more than 100 members of this class have been identified.<sup>62–64</sup>

(61) Callender, R.; Deng, H. *Annu. Rev. Biophys. Biomol. Struct.* **1994**, *23*, 215.  
 (62) Dunker, A. K.; Brown, C. J.; Lawson, J. D.; Iakoucheva, L. M.; Obradovic, Z. *Biochemistry* **2002**, *41*, 6573.  
 (63) Uversky, V. N.; Gillespie, J. R.; Fink, A. L. *Proteins* **2000**, *41*, 415.

$\alpha$ -Synuclein is a prototypical member of this class of proteins;<sup>23</sup> initial studies indicated that it has no distinguishable secondary structure by CD or NMR under physiological conditions but that it can adopt an  $\alpha$ -helical conformation in the presence of vesicles,<sup>65</sup> micelles,<sup>7</sup> 3 M trimethylamine oxide<sup>66</sup> or fluorinated solvents,<sup>23,33,34</sup> or  $\beta$ -sheet conformations in the presence of alcohols.<sup>67</sup> Interest has focused on discerning how the lack of well-defined structure can contribute to the physiological function of the protein, as well as on the nature of the biophysical properties that allow the conformational plasticity of the polypeptide to adopt different conformations in different environments. Further interest has developed in characterizing intermediate states in the aggregation pathway as evidence accumulates that these ill-defined aggregates or protofibrils may be responsible for the neurotoxicity of the amyloidogenic proteins.<sup>35,68,69</sup>

While natively unfolded proteins may lack static structures containing extended regions of  $\alpha$ -helix and  $\beta$ -sheet or  $\beta$ -strands, it is possible that they adopt an ensemble of dynamically interchanging secondary conformations. Because the standard tools of structural biology cannot be applied to these unfolded structures, other forms of spectroscopy have to be developed. The description of the “structure” of a natively unfolded protein requires the characterization of an ensemble of structures rather than the determination of a single conformation. Even more difficult is the characterization of structure in condensed “amorphous aggregates” as electron microscopy and atomic force microscopy reveal nearly featureless spherical aggregates.<sup>70–74</sup> Raman spectroscopy has the potential to characterize both forms of protein.

The structure of native globular proteins may be characterized by the  $\Phi$  and  $\psi$  torsion angles about each amino acid  $\alpha$ -carbon as indicated in Ramachandran plots. While natively unfolded proteins do not adopt single conformations, the steric constraints that limit native proteins to the  $\alpha$ -helical and  $\beta$ -structure regions of the Ramachandran plot remain.<sup>75</sup> This consideration suggests that in natively unfolded proteins these conformations will be preferred but that the position of each residue may fluctuate within or between these favored regions as part of the ensemble of structures. Thus, within this dynamic ensemble there may be at any moment several regions containing a few peptides that are all in  $\alpha$ -helical or  $\beta$ -strand Ramachandran space.

Different spectroscopic methods have different potentials in revealing characteristics of an ensemble of structures. NMR studies routinely provide a time-average of each individual resonance. For a fluctuating structure these data reflect an ensemble average for each residue. For  $\alpha$ -synuclein these studies

(64) Tompa, P. *Trends Biochem. Sci.* **2002**, *27*, 527.  
 (65) Davidson, W. S.; Jonas, A.; Clayton, D. F.; George, J. M. *J. Biol. Chem.* **1998**, *273*, 9443.  
 (66) Uversky, V. N.; Li, J.; Fink, A. L. *FEBS Lett.* **2001**, *509*, 31.  
 (67) Uversky, V. N.; Li, J.; Fink, A. L. *J. Biol. Chem.* **2001**, *276*, 10737.  
 (68) Walsh, D. M.; Hartley, D. M.; Kusumoto, Y.; Fezoui, Y.; Condron, M. M.; Lomakin, A.; Benedek, G. B.; Selkoe, D. J.; Teplow, D. B. *J. Biol. Chem.* **1999**, *274*, 25945.  
 (69) Volles, M. J.; Lansbury, P. T., Jr. *Biochemistry* **2003**, *42*, 7871.  
 (70) Fezoui, Y.; Teplow, D. B. *J. Biol. Chem.* **2002**, *277*, 36948.  
 (71) Olofsson, A.; Ostman, J.; Lundgren, E. *Clin. Chem. Lab Med.* **2002**, *40*, 1266.  
 (72) Conway, K. A.; Lee, S. J.; Rochet, J. C.; Ding, T. T.; Williamson, R. E.; Lansbury, P. T., Jr. *Proc. Natl. Acad. Sci. U.S.A.* **2000**, *97*, 571.  
 (73) Hoyer, W.; Antony, T.; Cherny, D.; Heim, G.; Jovin, T. M.; Subramaniam, V. *J. Mol. Biol.* **2002**, *322*, 383.  
 (74) Gorman, P. M.; Yip, C. M.; Fraser, P. E.; Chakrabarty, A. *J. Mol. Biol.* **2003**, *325*, 743.  
 (75) Ramakrishnan, C.; Ramachandran, G. N. *Biophys. J.* **1965**, *5*, 909.

have revealed regions in the N-terminus that have residual  $\alpha$ -helical propensity under physiological conditions.<sup>32</sup> By contrast, optical spectroscopies provide spectra that are linear combinations of the spectra for each conformation present since they provide an “instantaneous snapshot”.

The Raman spectra of polypeptide bonds, particularly the amide I vibration, are sensitive to the  $\Phi$  and  $\Psi$  angles of each residue as well as the H-bonding pattern and peptide–peptide dipole coupling. If spectra could be obtained of natively unstructured proteins that have been converted to largely  $\alpha$ -helical conformations/extended  $\beta$ -strands/the  $\beta$ -sheet typical of cross-beta fibrils, these spectra could serve as the basis for characterizing the propensity of natively unstructured proteins to occupy these different conformations. Isotope-editing could also provide a means of identifying the propensity of individual residues to adopt a given secondary conformation.<sup>54,76,77</sup>  $\alpha$ -Synuclein has provided an opportunity to pursue this characterization since it is a reasonably small protein that can adopt both  $\alpha$ -helical and  $\beta$ -sheet conformations under different conditions. Obtaining the Raman spectra of  $\alpha$ -synuclein under these conditions identifies basis spectra for each conformational state. These basis spectra are subsequently used to interpret changes in the Raman spectra as conformational responses to alterations in solution conditions.

**Assignment of Secondary Structure by Raman Spectroscopy.** Information regarding the protein secondary structure is reflected in the Raman amide I band (1640–1690  $\text{cm}^{-1}$ ) region and the amide III band (1230–1300  $\text{cm}^{-1}$ ) region.<sup>15,49,78</sup> The amide I region has a major contribution from C=O stretching ( $\nu_{\text{C=O}}$ ), while the amide III band contains a contribution from N–H in plane deformation. Analysis of the amide III band is complicated by overlapping bands from side chain vibrations,<sup>20</sup> and so our analysis focuses on the amide I peak. In  $\alpha$ -helical proteins and peptides the amide I band centers at  $\sim 1655 \text{ cm}^{-1}$ .<sup>60,79</sup> In Raman spectroscopy, this has served as a marker band for the contribution of ordered  $\alpha$ -helix<sup>3,5,10</sup> and was the only single-component contributor in the spectral decomposition by Sane et al.<sup>6</sup> In the fd phage coat protein, comprised of a protein that exists as a single kinked  $\alpha$ -helix,<sup>80</sup> the amide I band is centered at 1650–1652  $\text{cm}^{-1}$ .<sup>53</sup> The assignment of the  $\alpha$ -helix amide I band to a deconvoluted band at 1653  $\text{cm}^{-1}$  for  $\alpha$ -synuclein is confirmed by the presence of the amide I maxima at 1653–1655  $\text{cm}^{-1}$  in the presence of either SDS or HFIP. In both of these solvents the far UV–CD spectrum was characteristic of  $\alpha$ -helical proteins. Deconvolution of the spectrum in 25% HFIP indicated that the  $\alpha$ -synuclein was over 90%  $\alpha$ -helical. Thus, the Raman spectrum obtained under these conditions serves as a basis spectrum for regions of  $\alpha$ -helical content (regions that are temporarily in the dynamic ensemble and that may consist of only few residues) in natively unstructured proteins. A BWHH of 32  $\text{cm}^{-1}$  is observed for ‘tight’ well-formed structures and becomes broader when the  $\alpha$ -helix is less well formed,<sup>14</sup> either in the micelle solution or at lower concentrations of HFIP. The 1654  $\text{cm}^{-1}$  peak in Figure 4c may be from “loose” helices or a short sequence (<4) of

residues in  $\alpha$ -helical space and is consistent with the NMR observation of residues with  $\alpha$ -helical propensity.<sup>7</sup>

While the above observations demonstrate that amides in  $\alpha$ -helical space will be associated with amide I bands, between 1650 and 1655  $\text{cm}^{-1}$ , contributions could also arise from residues in  $\beta$ -space under appropriate conditions. Transition dipole coupling present in  $\beta$ -sheets results in strongly coupled amide I vibrations<sup>81</sup> that could contribute to this region. However, in well organized  $\beta$ -sheet structures, such as those observed in the Raman spectra of insulin fibrils, this band arising from the coupled in phase vibration of alternate carbonyl appears at 1630  $\text{cm}^{-1}$ . For this coupling of amide I vibrations to occur, at least three  $\beta$ -strands were required. In the extended  $\beta$ -strand and polyproline II structures, <sup>13</sup>C isotope editing<sup>82</sup> along with calculations have suggested that vibrational coupling is weak,<sup>59</sup> making a contribution from these conformations whose primary Raman signal is  $>1670 \text{ cm}^{-1}$ , minimal.

$\alpha$ -Synuclein can be induced to prefer  $\beta$ -sheet structure by the addition of methanol or ethanol.<sup>34</sup> These additions favor the subsequent aggregation of  $\alpha$ -synuclein into “cross-beta” fibrils. The alteration of the Raman spectrum induced by the addition of 25% methanol is thus characteristic of the formation of  $\beta$ -sheet structure. Characterizing  $\beta$ -strand contributions in Raman and infrared vibrational spectra is complicated by the strong vibrational coupling of the  $\nu_{\text{C=O}}$  modes and the contribution of transition dipole coupling. Recent quantum chemical modeling has characterized the lower frequency mode that predominates in the IR spectra with an out of phase stretching motion of successive carbonyls in a  $\beta$ -strand. A higher frequency mode,  $\sim 1665$ – $1670 \text{ cm}^{-1}$ , is identified as the in phase  $\nu(\text{C=O})$  of the interior carbonyls in the  $\beta$ -strands.<sup>81,83</sup> This mode provides the greatest contribution to the amide I intensity in the Raman spectra of  $\beta$ -structure. In *Bombix* silk, the prototypical  $\beta$ -sheet, the amide I region of the Raman spectrum is dominated by a single sharp peak at 1667  $\text{cm}^{-1}$ .<sup>48</sup> In the analysis of protein Raman spectra, similar assignments have been made with frequency maxima at 1669–1672  $\text{cm}^{-1}$ <sup>6,51</sup> and the amide I feature appears at  $\sim 1667 \text{ cm}^{-1}$  in amyloid cross-beta fibrils of insulin,<sup>11,14</sup> a silk moth chorion protein peptide,<sup>13,84</sup> and amyloid- $\beta$  peptide.<sup>12,13</sup> The appearance of a strong amide I band at 1667  $\text{cm}^{-1}$  as the methanol concentration increases (Figure 3c) is attributed to an increase in hydrogen-bonded  $\beta$ -sheet structure.

Under conditions where  $\alpha$ -synuclein is unstructured by other spectroscopic methods, the curve fitting of the Raman amide I band indicates a substantial contribution centered at 1681  $\text{cm}^{-1}$ . The assignment of the higher frequency features to random and turn conformations follows similar assignments for both IR<sup>79</sup> and Raman<sup>10</sup> spectroscopy. Tiffany and Krimm pioneered the idea of the presence of polyproline II structure in ionized polypeptides.<sup>85</sup> Polyproline II structure is a repeating extended  $\beta$ -strand structure without internal H-bonding. Recent work has favored polyproline II conformations both for short peptides<sup>86–88</sup>

(76) Decatur, S. M. *Biopolymers* **2000**, *54*, 180.

(77) Silva, R. A.; Barber-Armstrong, W.; Decatur, S. M. *J. Am. Chem. Soc.* **2003**, *125*, 13674.

(78) Williams, R. W.; Cutrera, T.; Dunker, A. K.; Peticolas, W. L. *FEBS Lett.* **1980**, *115*, 306.

(79) Dong, A.; Huang, P.; Caughey, W. S. *Biochemistry* **1990**, *29*, 3303.

(80) Marassi, F. M.; Opella, S. J. *Protein Sci.* **2003**, *12*, 403.

(81) Kubelka, J.; Keiderling, T. A. *J. Am. Chem. Soc.* **2001**, *123*, 6142.

(82) Woutersen, S.; Hamm, P. *J. Chem. Phys.* **2001**, *114*, 2727.

(83) Kubelka, J.; Keiderling, T. A. *J. Am. Chem. Soc.* **2001**, *123*, 12048.

(84) Iconomidou, V. A.; Chryssikos, G. D.; Gionis, V.; Vriend, G.; Hoenger, A.; Hamodrakas, S. J. *FEBS Lett.* **2001**, *499*, 268.

(85) Tiffany, M. L.; Krimm, S. *Biopolymers* **1972**, *11*, 2309.

(86) Eker, F.; Griebenow, K.; Schweitzer-Stenner, R. *J. Am. Chem. Soc.* **2003**, *125*, 8178.

(87) Shi, Z.; Olson, C. A.; Rose, G. D.; Baldwin, R. L.; Kallenbach, N. R. *Proc. Natl. Acad. Sci. U.S.A.* **2002**, *99*, 9190.

(88) Weise, C. F.; Weisshaar, J. C. *J. Phys. Chem. B* **2003**, *107*, 3265.



and in unstructured proteins.<sup>30,89</sup> A recent ROA study identified a significant contribution of polyproline II secondary structure in  $\alpha$ -synuclein.<sup>31</sup> Our Raman spectra are similar to the Raman spectra in this work and support the possibility that this high-frequency amide I feature is due to the presence of polyproline II structure. However, this band may also be due in part to  $\beta$ -strands, short sequences of residues in  $\beta$ -space that are not incorporated into  $\beta$ -sheets, as observed by Dong et al. in the Raman spectra of insulin.<sup>90</sup>

To further characterize the band at  $\sim 1681\text{ cm}^{-1}$ , Raman spectra of peptides known to adopt a polyproline II structure were obtained. Figure 6 shows the Raman spectra of poly-L-lysine and poly-L-glutamic acid at different pHs. At pH 12, the amide I band for poly-L-glutamic acid appears at  $1674\text{ cm}^{-1}$ . A similar band appeared at  $1671\text{ cm}^{-1}$  for poly-L-lysine at low pH (pH = 3.5). These two polypeptides, when the charged side chains repel each other, are believed to attain a structure similar to polyproline II.<sup>85</sup> Barron and co-workers determined the ROA band of these peptides, compared the ROA bands of  $\alpha$ -synuclein, and concluded that the structure of  $\alpha$ -synuclein has similarities to the polyproline II structure of polyglutamic acid at high pH.<sup>31</sup>

**Interpretation of  $\alpha$ -Synuclein Raman Spectra.** A minimal band fitting of the amide I band is proposed for  $\alpha$ -synuclein and, by cautious extrapolation, to other natively unfolded proteins.  $\alpha$ -Helical segments, both extended and short fragments, have a Raman signature band at  $\sim 1652\text{ cm}^{-1}$  with a BWHH of  $\sim 30\text{ cm}^{-1}$ . Significantly increased bandwidths correspond to residues in shorter and looser sequences.  $\beta$ -Sheet residues, implying the presence of interstrand H-bonding, contribute to a band at  $\sim 1667\text{ cm}^{-1}$ , and residues in  $\beta$ -space but not within sheets including extended and polyproline II conformations are observed in the  $1671\text{--}1680\text{ cm}^{-1}$  region. Band fitting the amide I spectrum to these three frequency regimes permits the detection of populations of different secondary structures and can identify changes in the relative populations induced by varying solvent or other experimental conditions. Analysis of the amide I spectrum of NAC suggests that this hydrophobic region of  $\alpha$ -synuclein has a decreased contribution from  $\alpha$ -helical conformations that is compensated by increases in both the  $\beta$ -sheet and extended conformations. This region has been proposed to be the nucleation site for fibril formation, and our analysis indicates that under physiological conditions it has a greater propensity to adopt conformations in  $\beta$ -space.<sup>91</sup> Identifying the propensities of individual residues within the peptide of protein could be determined by site-specifically labeling the amide carbonyl of interest.

The three-component band fitting permits the effect of methanol on the conformation of  $\alpha$ -synuclein to be inferred. In aqueous solution there are substantial populations of residues in both  $\alpha$ - and  $\beta$ -space, but the  $\beta$ -structure is present in extended chains and not sheets as the contribution of the band at  $1667\text{ cm}^{-1}$  is  $<15\%$ . The increased BWHH of the low-frequency ( $1650\text{ cm}^{-1}$ ) component suggests that the helices are not extended and may be subject to considerable variation in their conformation. The presence of an  $\alpha$ -helical contribution to the

Raman spectrum is consistent with the NMR observation of a tendency for the N-terminus to have  $\alpha$ -helical characteristics.

The structure in intermediate methanol concentrations is of interest as these concentrations accelerate fibril formation.<sup>34</sup> The intensity of the low-frequency band ( $1650\text{ cm}^{-1}$ ) decreases, suggesting an overall decrease in  $\alpha$ -helical composition. The narrowing of the bandwidth suggests that the remaining  $\alpha$ -helical residues are present in more extended and possibly more rigid  $\alpha$ -helices. This is consistent with the qualitative appearance of the CD spectrum, which suggests the continuing presence of  $\alpha$ -helix under these conditions. The increase in the  $\beta$ -sheet band at  $1667\text{ cm}^{-1}$  is apparent, suggesting the significant development of  $\beta$ -sheet structure. The appearance of  $\beta$ -sheet is correlated with the appearance in the amide III region band of a sharpened band appearing at  $1240\text{ cm}^{-1}$ . At higher methanol concentrations ( $>25\%$ ) the Raman spectrum suggests that the structure is predominantly  $\beta$ -sheet, with minimal contributions of  $\alpha$ -helical or extended structure, and serves as a basis structure. The decrease in extended or polyproline II structure is consistent with the notion that an aqueous solvation shell stabilizes the polyproline II conformation,<sup>92</sup> which can be disrupted by the addition of a cosolvent.<sup>93</sup>

In contrast to the effect of methanol, HFIP induces the development of an  $\alpha$ -helical conformation in  $\alpha$ -synuclein. At 25% HFIP the structure is mostly  $\alpha$ -helical, as evidenced both by the CD and Raman spectra, where the amide I is centered at  $1653\text{ cm}^{-1}$  and the BWHH is  $\sim 33\text{ cm}^{-1}$ , and with minimal contributions from higher frequency features. The bandwidth can be compared to insulin,<sup>14</sup> where the  $\alpha$ -helical Raman band has a BWHH of  $\sim 32\text{ cm}^{-1}$ . The Raman spectrum of  $\alpha$ -synuclein in SDS has a broader feature at  $1654\text{ cm}^{-1}$ , suggesting that under these conditions there are variations in solvation and/or "tightness" of the  $\alpha$ -helix.

**Analysis of Natively Unfolded Proteins.** The Raman amide I spectra of natively unfolded proteins are less complex than that of structured proteins for two main reasons. The unfolded proteins have fewer turns than natively folded proteins, suggested by their larger hydrodynamic radii. The conformation of the four residues in each  $\beta$  turn varies and results in a broad dispersion of amide I frequencies. The absence of a hydrophobic core in unstructured proteins results in less variation in amide bond solvation, again minimizing the dispersion of amide I frequencies. Removing these two sources of variation leaves backbone conformation as a predominant contributor to the amide I spectral dispersion. Both the peak positions and the spectral widths of the fitted bands provide information on the ensemble of structures. In comparing the amide I bands for phosvitin,  $\alpha$ -casein, and  $\beta$ -casein it is apparent that phosvitin contains a significantly more extended structure. The presence of the negative charges on the phosphorylated residues results in a charge repulsion like that in polyglutamate and polylysine that favors the extended structure. In contrast, the caseins have significant propensities to contain  $\alpha$ -helical region as evidenced by the significant contribution of the  $1653\text{ cm}^{-1}$  bands.  $\beta$ -Casein may be distinguished from  $\alpha$ -casein by the increased contribution of the band at  $1670\text{ cm}^{-1}$  indicative of an increased contribution from residues adopting conformations in  $\beta$ -space.

(89) Shi, Z.; Woody, R. W.; Kallenbach, N. R. *Adv. Protein Chem.* **2002**, *62*, 163.

(90) Dong, J.; Wan, Z. L.; Chu, Y. C.; Nakagawa, S. N.; Katsoyannis, P. G.; Weiss, M. A.; Carey, P. R. *J. Am. Chem. Soc.* **2001**, *123*, 7919.

(91) Han, H.; Weinreb, P. H.; Lansbury, P. T., Jr. *Chem. Biol.* **1995**, *2*, 163.

(92) Han, W.-G.; Jalkanen, K. J.; Elstner, M.; Suhai, S. *J. Phys. Chem. B* **1998**, *102*, 2587.

(93) Eker, F.; Cao, X.; Nafie, L.; Huang, Q.; Schweitzer-Stenner, R. *J. Phys. Chem. B* **2003**, *107*, 358.

**Comparison of  $\alpha$ -Synuclein Raman and CD Spectra.** Far UV-CD spectra of proteins reflect the chiral environment of the amide chromophores, thereby requiring an extended region of secondary structure to be observed. However, vibrational spectroscopy reflects the properties of individual peptide bonds, a more localized phenomenon, that responds to the immediate  $\phi$  and  $\Psi$  dihedral angles and its H-bonding status. Ozdemir et al.<sup>94</sup> demonstrated that UV resonance Raman spectroscopy was capable of detecting short  $\alpha$ -helical segments not observed by CD. This difference between extended and local responsiveness provides a rationale for the absence of helical structure in the CD spectrum of  $\alpha$ -synuclein in aqueous solution, while the Raman spectrum suggests  $\sim 48\%$  helical structure. Both observations can be accommodated if the  $\alpha$ -helical residues occur in such short stretches that the contribution to the CD spectrum is minimized. At increasing MeOH concentrations, the component analysis of the CD spectra using different programs failed as strikingly different results were obtained. The main problem is that all of the methods of CD analysis suggest the presence of substantial  $\alpha$ -helical components at 25% MeOH. Under the same conditions the Raman spectra suggest that the fraction of the protein that is  $\alpha$ -helical decreases dramatically when the MeOH concentration increases above 17.5%. Visual observation of the CD spectra does not reveal what aspect of the CD spectrum is generating the  $\alpha$ -helical assignment as there does not appear to be an enhanced negative helicity at 222 nm. Since standard globular proteins contribute to the calibration structures for

(94) Ozdemir, A.; Lednev, I. K.; Asher, S. A. *Biochemistry* **2002**, *41*, 1893.

CD analysis software, it is not surprising that there are aspects of the natively unfolded structure of  $\alpha$ -synuclein that are not well correlated.

### Summary and Prospectus

$\alpha$ -Synuclein has provided a favorable system for secondary structural characterization by Raman spectroscopy since solution conditions were identified where either  $\beta$ -sheet or  $\alpha$ -helical conformations predominated, permitting basis spectra for both conformations to be obtained. Using the Raman signatures of amide I bands at  $1653\text{ cm}^{-1}$  for  $\alpha$ -helix,  $1667\text{ cm}^{-1}$  for  $\beta$ -sheet, and  $1674\text{--}1685\text{ cm}^{-1}$  for extended  $\beta$ -strand and polyproline II structure, a band-fitting approach suffices to identify the presence, or change in relative contribution, of these secondary structural elements. These spectroscopic features can be used for kinetic studies of  $\alpha$ -synuclein's conformational changes that occur prior to fibrillization, to structurally characterize intermediates and aggregates that form during the fibrillization process,<sup>72,95</sup> and to determine the structure of  $\alpha$ -synuclein aggregates that form in vivo.<sup>13</sup> Because individual peptide bonds can be identified by isotopic labeling, the potential exists to extend this characterization to specific residues of interest in the  $\alpha$ -synuclein sequence.<sup>54</sup>

**Acknowledgment.** This work was supported by grants from the Alzheimer's Foundation, IIRG-02-4384 (to M.G.Z.), and the NIH, AG14249 (to V.E.A.) and GM 54072 (to P.R.C.).

JA0356176

(95) Uversky, V. N.; Lee, H. J.; Li, J.; Fink, A. L.; Lee, S. J. *J. Biol. Chem.* **2001**, *276*, 43495.